BJR

https://doi.org/10.1259/bjr.20170644

Received: 29 August 2017 | Revised: 14 November 2017 | Accepted: 23 November 2017

Cite this article as:
Silva M, Milanese G, Seletti V, Ariani A, Sverzellati N. Pulmonary quantitative CT imaging in focal and diffuse disease: current research and clinical applications. *Br J Radiol* 2018; **91**: 20170644.

REVIEW ARTICLE

Pulmonary quantitative CT imaging in focal and diffuse disease: current research and clinical applications

[1]MARIO SILVA, MD, PhD, [1]GIANLUCA MILANESE, MD, [1]VALERIA SELETTI, MD, [2]ALARICO ARIANI, MD and [1]NICOLA SVERZELLATI, MD, PhD

[1]Department of Medicine and Surgery (DiMeC), Section of Radiology, Unit of Surgical Sciences, University of Parma, Parma, Italy
[2]Department of Medicine, Internal Medicine and Rheumatology Unit, University Hospital of Parma, Parma, Italy

Address correspondence to: Prof Nicola Sverzellati
E-mail: *nicola.sverzellati@unipr.it*

ABSTRACT

The frenetic development of imaging technology—both hardware and software—provides exceptional potential for investigation of the lung. In the last two decades, CT was exploited for detailed characterization of pulmonary structures and description of respiratory disease. The introduction of volumetric acquisition allowed increasingly sophisticated analysis of CT data by means of computerized algorithm, namely quantitative CT (QCT). Hundreds of thousands of CTs have been analysed for characterization of focal and diffuse disease of the lung. Several QCT metrics were developed and tested against clinical, functional and prognostic descriptors. Computer-aided detection of nodules, textural analysis of focal lesions, densitometric analysis and airway segmentation in obstructive pulmonary disease and textural analysis in interstitial lung disease are the major chapters of this discipline. The validation of QCT metrics for specific clinical and investigational needs prompted the translation of such metrics from research field to patient care. The present review summarizes the state of the art of QCT in both focal and diffuse lung disease, including a dedicated discussion about application of QCT metrics as parameters for clinical care and outcomes in clinical trials.

INTRODUCTION

The modern CT scanner has excellent spatial and temporal resolution for anatomical evaluation *in vivo*. The ability to derive quantitative CT (QCT) imaging provides a non-invasive mean for direct visualization, characterization and quantification of anatomic structures, as well as for speculation about pathophysiological processes of pulmonary diseases.[1]

There is clearly interest in optimizing the role of QCT for application of its objective metrics, for instance in clinical trials and lung cancer screening.[2–4] Indeed, QCT techniques for characterization of interstitial lung disease (ILD), chronic obstructive pulmonary disease (COPD), as well as focal lesions (*e.g.* lung nodules), have been progressively developed, validated and refined over the past 20 years.

The purpose of the present review article is to summarize major QCT advances in both focal findings and diffuse lung disease, either in research or routine realms.

DETECTION AND CHARACTERIZATION OF PULMONARY NODULE

State of the art

Computer-aided detection (CAD) of pulmonary nodule was progressively introduced, improved and validated for optimization of radiologist reading.[5] In particular, CAD has been massively tested within lung cancer screening trials, where it could be optimized for both sensitivity and, notably, positive-predictive value (*e.g.* reduction of false-positive CAD findings is a major issue for optimal efficiency of the system).[6–8] CAD can act as first, second or concurrent-reader.[9] The second reader approach shows the highest sensitivity at the cost of a greater reading time compared to the concurrent reader.[9–16]

CAD has been evaluated for the detection of both solid and subsolid nodules.[17] Sensitivity of CAD for solid nodules ranged from 38 to 100%.[18–22] Sensitivity for the detection of subsolid nodules of the first CAD software was poor[23] and currently shows a wide range between 54%[24] and above 70%.[17,25,26] This high heterogeneity derives from the technical differencesf the CAD systems commercialized by

various manufacturers as well as from different studies' methodologies.[14,27] Subsolid nodules are less frequent than the solid ones, nevertheless, they show higher incidence of lung neoplasms,[28] hence, it is mandatory that CAD be validated before its implementation in this subset of nodules.

CAD provides the radiologist with semi-automatic metrics driving the nodule management, such as volume and volume doubling time, which are more accurate than manual diameter.[29,30] Noteworthy, volumetric measurements and volume doubling time are particularly useful for the evaluation of size change during follow-up.[31] Nevertheless, it cannot be overemphasized that variation occurs also for semi-automatic volumetry of nodules by CAD, notably as a function of size[32] and in association with inspiratory effort.[33] It was proposed that 25% increase be an accurate threshold to define nodule growth in the follow-up of indeterminate solid nodules surrounded by aerated parenchyma (more limitations apply to nodules abutting vessels, bronchi and pleura).[34,35] A combination of volume and density is used to calculate the mass and the mass doubling time of subsolid nodules (Figure 1).[36] However, such metrics are not widespread,[37] partly because of the variability between different CAD software (even between different versions of the same software) that hampers longitudinal reproducibility (*e.g.* when measurements are performed in different radiology departments during follow-up).[32,38] The suggestion is to analyse the complete data set of CT time points with the same software at the time of the most recent CT scan, eventually with its most recent software version.

Clinical application

CAD aims to reduce false-negative scans,[13,39,40] which are associated with the lone visual reading,[41] thus improving sensitivity.[14,42] For instance, in a series of 400 low-dose CTs with 151 true-positive findings, 5 were missed by CAD while 33 by the two reading radiologists.[21] However, in the current clinical daily practice, CAD are not commonly used because of the drawback of a high rate of false-positive findings requiring radiologists' interaction[5,43,44] and the need for data transfer to a dedicated workstation. Noteworthy, lung cancer trials showed the usefulness of CAD for the semi-automated detection and measurement of nodules.[6,8,45] In keeping with the results of such large studies, it is believed that CAD will progressively be integrated also in clinical practice, increasing the sensitivity of radiologists for lung nodules.

Application in scientific investigation and clinical trials

The major issue of nodule management comes with the large amount of clinically silent lesions (*e.g.* benign, premalignant or malignant with indolent behaviour). Interobserver variability is the main limitation in objective assessment of nodule risk, yet, there are computerized alternatives for such task, also called radiomics. Radiomics is the high-throughput extraction of image features imperceptible for the human eyes,[46] such as pixel values, variation of those values within a region of interest (ROI) and edge strengths.[47]

Figure 1. (a–i) CAD segmentation of subsolid nodule during a 4-year active surveillance. The semi-automatic segmentation of pulmonary nodule provides several metrics that can be used for standardized characterization and management. Noteworthy, the longitudinal assessment of subsolid nodule takes advantage of volumetric measurement of density, which was proposed for optimal stratification of nodule growth, also known as mass doubling time. From right to left, the same non-solid nodule segmented at baseline (a–c), after 2 years (middle column: d–f), and after 4 years (g–i) with progressive increase in growth rate according to MDT. For each time point the segmentation is rendered in axial (a, d and f), coronal (b, e and h) and sagittal plane (c, f and i). The MDT of this non-solid nodule rose from 1562 days at the 2-year LDCT to 350 days at the 4-year LDCT, reflecting a progressive increase in growth rate. CAD, computer-aided detection; LDCT, low-dose CT; MDT, mass doubling time.

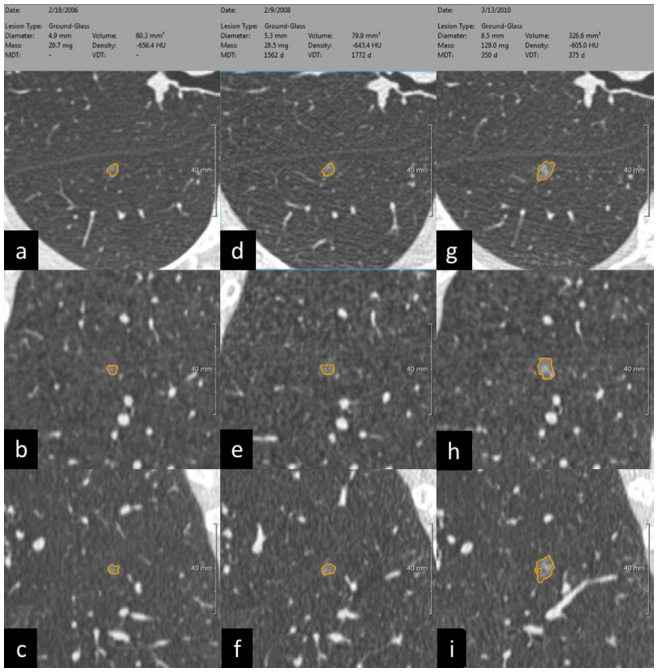

Currently, there are a number of software available for texture analysis (TA), each of them capable to extrapolate and evaluate different groups of radiomic features.[48] Radiomics works in multistep fashion composed of subsequent processes, namely: image acquisition, delineation of ROIs and extraction and analysis of features.[49] Noteworthy, features can be extracted with a semi-automated method reducing the number of manual inputs[50] and this approach might be beneficial if TA will be available in the clinical workflow.

Radiomic features extraction currently suffers from a significant inter-reader variability related to the selection of ROI.[51] TA was shown to be capable of predicting patient outcome based on CT data sets acquired with different scanning parameters[52]—the latter representing a frequent work setting— however, there is evidence about significant variability among CT data sets reconstructed with different algorithms.[51,53,54] Hence, future studies should investigate whether different scanning protocols can reliably be used for the TA-based stratification of patients. The

consistency of radiomic features extracted from CT data sets obtained by different scanners will be particularly beneficial for clinical application as radiologists are frequently asked to compare CT studies acquired from different hospitals.

TA was evaluated to determine if radiomic features could differentiate between lung cancer and benign nodules,[55] as well as between transient and persistent part-solid nodules[56] or pre-invasive and invasive part-solid nodules.[57,58] In patients suffering from lung cancer, TA could non-invasively monitor changes in tumour heterogeneity in the early phase of therapy[59] to potentially provide objective biomarkers[31,60] for prediction of treatment response and survival.[30,46,51,61–66] Furthermore, TA is increasingly investigated to stratify the risk of distant metastases from lung cancer[52] as well as to provide *in vivo* non-invasive differentiation between histological types of lung cancer,[67] we hope future developments will supply robust metrics for this purpose.

OBSTRUCTIVE PULMONARY DISEASE

The heterogeneous framework of obstructive pulmonary disease can be biased on pulmonary function tests (PFTs). Conversely, quantitative imaging can detail abnormalities and differentiate between parenchymal and bronchial disease,[68,69] yet its validation for clinical application can be further demonstrated. CT is not recommended as part of the routine evaluation of obstructive pulmonary disease, nevertheless it can be employed in the phenotypization of chronic obstructive pulmonary disease (COPD),[4] therapeutic planning for emphysema,[70] characterization of asthma,[71] early detection of bronchiolitis obliterans syndrome after transplantation (*e.g.* bone marrow, lung)[72] and even in paediatric obstructive diseases (*e.g.* cystic fibrosis, bronchopulmonary dysplasia).[73,74] The characterization of parenchyma and airway in obstructive pulmonary diseases has been anatomically and functionally covered by volumetric and multiphase CT acquisition.[75,76]

State of the art

Parenchymal quantification

Pulmonary texture in obstructive lung disease shows relatively low tightness compared to normal lung because of air abundance. Air abundance can be caused either by tissue loss (*e.g.* emphysema) or by functional limitation to air outflow (*e.g.* air trapping), oftentimes by a combination of them. The more the air the lower the pulmonary density, which can be quantified by volumetric segmentation of the lung and arithmetic analysis of density histogram (Figure 2). Densitometric quantification includes absolute thresholding and relative distribution of voxel density.

Pulmonary density is highly influenced by the respiratory phase;[77] this characteristic offers the opportunity for morpho-functional quantification of the lung.

On inspiratory scans, emphysema is conventionally attributed to areas of lung with density < −950 Hounsfield unit,[78] moreover, it is indirectly related to the lowest 15th percentile (P15)[79] (Figure 2). It cannot be overemphasized that lung density is also

Figure 2. (a–d) Density histogram for computation of parenchymal metrics. Axial CT images of a patient with upper lobe predominant emphysema (a, b). The density histogram (c) summarizes the distribution of parenchymal density (white line: both lungs). Dedicated representation of individual lobar density histograms provides quantitative differences between lobes (red line: right upper lobe; green line: right lower lobe) for objective assessment of emphysema heterogeneity and selection of the most appropriate treatment (*e.g.* endobronchial valves *vs* endobronchial coils). Numeric output is automatically computed by the software (d) and displayed according to whole lung characteristics or according to the selected lobes (*e.g.* right and left lung or individual lobes). Quantitative metrics that can be extracted from the histogram include lung volume, mean lung density, weight, density percentiles (in the present table, the lowest 15th percentile is reported, P15), density mode (the most represented density value within the entire lung, Pk) and volume of lung parenchyma with density below a predefined threshold (in the present table, the relative volume of lung with density < −950 HU is reported as a measure of emphysema, LAV, low attenuation volume). HU, Hounsfield unit; MLD, mean lung density; Vol. volume; Wt., weight.

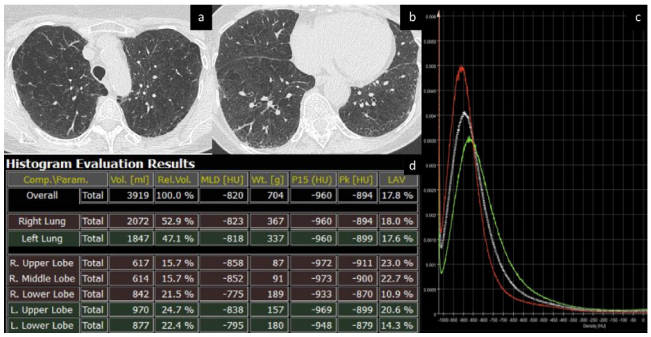

Comp.\Param.		Vol. [ml]	Rel.Vol.	MLD [HU]	Wt. [g]	P15 [HU]	Pk [HU]	LAV
Overall	Total	3919	100.0 %	-820	704	-960	-894	17.8 %
Right Lung	Total	2072	52.9 %	-823	367	-960	-894	18.0 %
Left Lung	Total	1847	47.1 %	-818	337	-960	-899	17.6 %
R. Upper Lobe	Total	617	15.7 %	-858	87	-972	-911	23.0 %
R. Middle Lobe	Total	614	15.7 %	-852	91	-973	-900	22.7 %
R. Lower Lobe	Total	842	21.5 %	-775	189	-933	-870	10.9 %
L. Upper Lobe	Total	970	24.7 %	-838	157	-969	-899	20.6 %
L. Lower Lobe	Total	877	22.4 %	-795	180	-948	-879	14.3 %

a function of tissue inflammation as it was shown in former smokers.[80] Therefore, lung density should always be interpreted within the appropriate pathophysiological context. It was proposed that emphysema quantification be integrated with lung mass for comprehensive depiction of a multiphase disease that might begin with active inflammation (higher density) and evolve towards irreversible tissue depletion (lower density). Washko reported that lung mass increasingly dropped from GOLD 1 to GOLD 4 (global initiative for chronic obstructive lung disease), and it predicted FEV1 (forced expiratory volume) decline in a large population of smokers (current or former).[81]

Volumetric expiratory scan for assessment of lung parenchyma is acquired at the end of expiration. Such acquisition was relatively challenging in the past, yet, it is currently made much easier by scanners with large arrays of detectors (*e.g.* 64 or more) that allow fast scan of the whole chest (scan time <5 s). Expiratory scan is useful to assess functional parenchymal change caused by obstructive small airway disease, namely air trapping. The densitometric parameters for quantification of air trapping include the relative area of lung < −856 Hounsfield unit on expiratory scan[82] and the ratio between expiratory and inspiratory mean lung density.[83] However, these two metrics have potential bias due to the heterogeneity of parenchymal densitometry at different

Figure 3. (a-d) Parametric response mapping for topographic densitometric categorization of parenchyma into normal lung, air trapping and emphysema in COPD. Volumetric inspiratory (a) and expiratory (b) CTs are warped together for quantitative analysis of densitometric clusters by means of parametric response map (c): Insp > −950 HU and Exp > −856 HU (normal lung), Insp > −950 and Exp < −856 HU (SAD) and Insp < −950 and Exp −856HU (emphysema). The native CT data set (d) is overlaid by colour-coded volumetric representation of the densitometric categories that allow topographic description of pulmonary disease (green, normal lung; yellow, air trapping; red, emphysema). The present COPD case shows the coexistence of air trapping and emphysema, which are objectively apportioned by the b-phase densitometric quantification with evidence of airway predominant disease. COPD, chronic obstructive pulmonary disease; HU, Hounsfield unit; SAD, small airway disease.

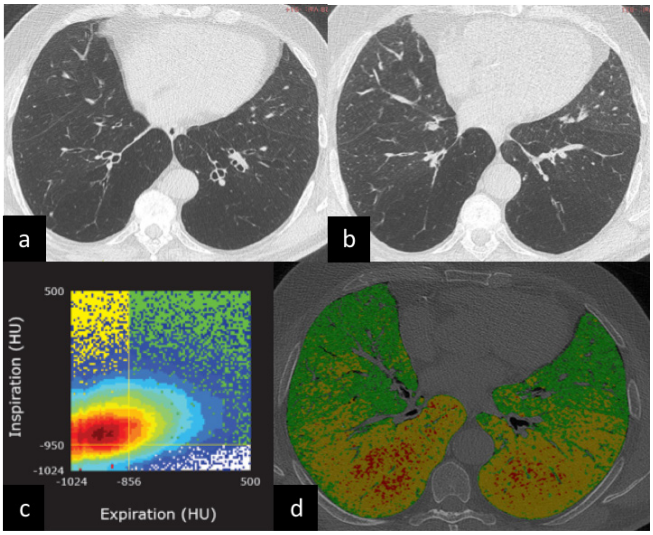

lung volumes, notably because air trapping and emphysema may be admixed.[84] Volumetric non-rigid registration of inspiratory and expiratory scan overcomes such limitation because it allows biphase characterization of each voxel, and is particularly interesting for quantification of air trapping. This approach was named parametric response mapping (PRM) when used to define density clusters for topographic categorization of parenchyma into normal lung, air trapping and emphysema[85] (Figure 3). A similar registration was used to simulate the local dynamic volume change. Bodduluri reported biomechanical CT descriptors of air trapping in association with patient outcome in a large COPD population.[86] Nonetheless, it should be realized that there is a normal range of air trapping even in young healthy subjects, which should be acknowledged for clinical application of QCT.[87,88]

Airway quantification

Quantitative analysis of the airway follows the preliminary processing step of bronchial tree segmentation and isolation of three-dimensional airway model[89,90] (Figure 4a–c). Airway is usually quantified according to its generation, and the generation-specific mean can be calculated throughout the entire lung,[91] nonetheless, Gupta et al reported that a single bronchus might

Figure 4. (a–d) Direct and indirect quantification of airway. Airway segmentation from trachea to intrapulmonary bronchi and stretched view of a selected airway in the right lower lobe (a); oblique axial reformatting of bronchial structure with direct automatic segmentation lumen diameter (LD: 4.6 mm), wall thickness (WT: 1.0 mm) and relative surface of wall compared to total airway surface (wall area, WA%: 52.1). Volumetric reconstruction of airway segmentation (c) for automatic direct measurement of all airways for indirect calculation of Pi10 by means of regression line derived from plotting of internal perimeter and square root of wall area of airways with internal perimeter <20 mm (d).

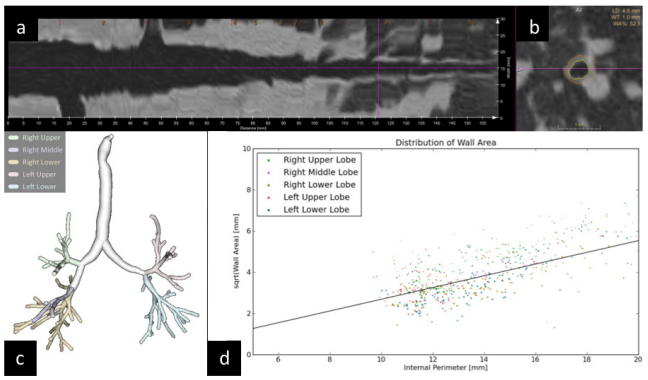

be representative.[92] Direct characterization of airway is feasible for several bronchial generations,[93] yet, direct QCT metrics are widely accepted up to fifth generation.[94,95] Direct quantification of airway includes lumen diameter and area, wall thickness and area, relative area of wall (obtained by the ratio between area of the wall and total area of the airway at a given section) and density of the airway wall.[96] Smaller airway can be indirectly quantified by the regression line between the square root of the airway wall area and the internal perimeter of the airway: the so called Pi10 that reflects wall conspicuity in airway with internal perimeter of 10 mm (broadly 3 mm of internal diameter) (Figure 4d). The variability and potential bias of airway metrics are significant and include lung volume, age and transient inflammation.[91,97] For this reason, the clinical application of airway QCT is still to be validated.[4] Pi10 is deemed the most consistent among airway metrics, albeit only when calculated on a minimum of 12 subsegmental bronchi.[98] Beyond size of bronchial components, also density was investigated and potential association with mast cell infiltration was found in asthmatic patients.[99]

Expiratory scan is still an issue for direct quantification of airway. Preliminary experiences suggested that more severe asthma might be associated with increased airway stiffness at third and fourth generation bronchi.[100] However, more analysis is needed to have a clear picture on the consistency of this observation.

Vascular quantification

Vascular quantification is relatively complex task in quantitative imaging of the lung. Quantitative metrics of pulmonary vascular volume have been recently proposed and are utmost promising to fill the gaps between morphological descriptors and physiology. Diaz showed that the broncho-arterial ratio is increased in smokers because of a relative reduction in vessel size.[101] More

quantitative studies showed characteristic vascular pruning of small pulmonary arteries[102] and reduction of lung perfusion assessed by contrast-enhanced dual-energy spectral CT.[103] The latter was first shown to detect perfusional defects in pulmonary embolism, with increasing degree of enhancement from occlusive to non-occlusive clots.[104] The spectral imaging for quantification of small pulmonary vessels is now being approached by extremely preliminary experience for detection of lung susceptibility to vasodilators in healthy smokers with emphysema,[103] yet, its application still yields some degree of variability (*e.g.* cardiac ejection rate, physiological gradients and scanning conditions) and artefacts (*e.g.* beam hardening, cardiac motion) that prevent such technique in the routine of COPD.[105,106] The role of vascular disease in the complex pathogenesis of COPD needs to be further investigated from different perspectives, either as a cause or a consequence of lung tissue depletion, and in association with cardiovascular function. Along the cardiopulmonary functional cascade, left ventricle filling and systemic blood delivery progressively decrease according to emphysema extent and airflow obstruction, as it was shown in a large cohort of COPD patients.[107]

Clinical application

The hardest effort towards standardization of imaging data set (acquisition and reconstruction) is mandatory for clinical application of quantitative imaging.[108–110] In particular, continuous change in protocol acquisition for dose reduction and related evolution in reconstruction algorithm should be accounted.[111,112]

The clinical application of quantitative imaging looks now closer than ever, in particular in tertiary centres where multidisciplinary teams optimally merge information from physiology, symptoms, imaging and therapeutic options.

Treatment of emphysema

Lung volume reduction (LVR) is a therapeutic option to improve pulmonary mechanics in severe emphysema. Techniques of LVR include endobronchial valves (EBV), endobronchial coils and surgery (LVRS). Regional quantification of emphysema by CT is paramount for the planning of LVR.[70,113] Emphysema distribution pattern and fissures integrity are pivotal for prediction of treatment efficacy.

EBVs can be used in both upper and lower predominant emphysema and are the less invasive technique, yet their selection criteria are extremely strict: fissure integrity >90% for prediction of collateral ventilation (major contraindication to EBV), heterogeneity of emphysema distribution between lobes (>15% difference in emphysema extent between ipsilateral lobes), emphysema >40% in the target lobe[114] (Figure 2). Furthermore, CT is extremely useful also for measurement of bronchial lumen and tailoring of EBV size. In the follow-up, CT can quantify the lobar volumetric reduction in treated lobes and the relative expansion of healthier lobes.

If EBV requirements are not met, endobronchial coils or LVRS can be considered. LVRS should be proposed only for upper lobe predominant emphysema. Both techniques are substantially irreversible, hence, they are preceded by a CT-based quantification of residual volume for estimation of post-procedural pulmonary function.[115] For this purpose, the integration of lung damage by CT quantification and perfusion scintigraphy provides the best prediction of clinical outcome.[116]

COPD phenotypization

The relative contribution of airway and parenchymal disease varies substantially in COPD, and determines prognosis and therapeutic response. PFTs have limitation in differentiating between phenotypes,[68] thus, patients with the same GOLD stage may present substantial clinical differences. Conversely, the literature on QCT increasingly supports the substantial amount of functional information that can be extracted from CT for phenotypization of COPD, even in case of mild to moderate disease.[117,118] Integration of visual and quantitative CT assessment permits categorization of COPD into emphysema predominant subtypes (proposed five different patterns) and airway-predominant subtypes (proposed two patterns).[119] Most subjects with emphysema have significant airway disease, conversely, a proportion of COPD subjects have minimal emphysematous lung (<6% of lung with density < −950 HU on inspiratory CT) and predominant airway disease.[119] PRM for objective estimation of normal lung, air trapping and emphysema appears to be the most promising QCT tool for clinical phenotypization of COPD, with potential application in longitudinal follow-up (Figure 3).[120,121]

Bronchiolitis obliterans syndrome in transplanted patients

Bronchiolitis obliterans syndrome is seen after lung or bone marrow transplantation.[72,122] It is diagnosed by spirometry, though there is lack of clinical tools to identify the degree of small airway obstruction. Quantification of functional small airways disease by PRM was shown to offer prognostic stratification in transplant recipients with spirometric decline.[72,122] In particular, PRM-quantified air trapping >30% after lung transplant could outrank subjects with shorter survival among patients with decline in lung function.[72]

Application in scientific investigation and clinical trials

Lung imaging is now being employed to provide quantitative assessment of morphology and function in scientific investigation. The utmost ability of imaging for non-invasive quantitative *in vivo* assessment of obstructive lung diseases increasingly provides imaging biomarkers as outcome measures in clinical trials.

Large longitudinal prospective trials recruited thousands of patients with and without COPD to undertake deep analysis about the clinical, functional, imaging and genetic framework of this syndrome.[123–125] These powerful trials represent the cornerstone of QCT investigation in COPD and provide massive data for its translation to clinical practice.[4,126,127] Major reports from these studies include regional disease progression,[121] QCT metrics associated with COPD exacerbations,[127,128] quantification of cardiovascular disease in COPD,[129] QCT stratification of smokers without COPD,[86,130] variability of parenchymal QCT

Figure 5. (a–c) Asthma phenotypes according to QCT cluster. Volumetric model of segmented airway and specific quantitative analysis of the right upper lobe apical segmental bronchus (RB1) on cross-section (insets). The airway metrics were normalized to the body surface area for definition of QCT clusters of asthma according to wall volume (WV) and lumen volume (LV). The three clusters are defined as follows: (a) cluster 1 with increased WV and LV, decreased percentage WV and severe air trapping; (b) cluster 2 with minor central airway remodelling, moderate air trapping and low response to bronchodilator; (c) cluster 3 reduced WV and LV, increased WV percentage and severe air trapping on CT. Figure reproduced under a Creative Commons license (CC BY) from Gupta S. et al, *J Allergy Clin Immunol*. 2014 Mar;133[3] :729–38.e18. https://doi.org/10.1016/j.jaci.2013.09.039. LV, lumen volume; QCT, quantitative CT; WV, wall volume.

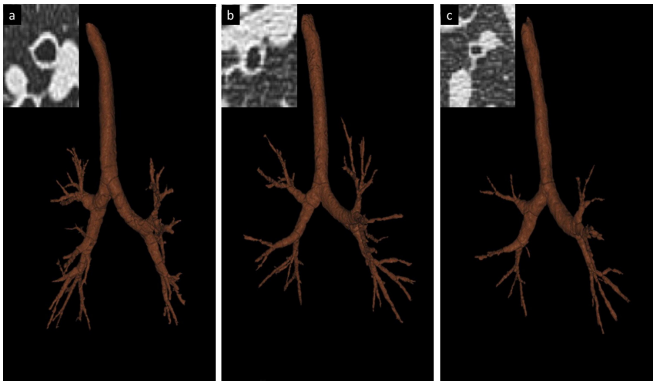

metrics according to smoking status[80] and standardization of CT protocol for multicentre application of QCT phenotypes.[108]

Emphysema

Emphysema is irreversible disease by definition, and in some cases it is relatively fast progressive. It is the case of α−1 antitrypsin deficiency where parenchymal tissue is actively disrupted as a consequence of reduced protease inhibition. QCT of lung parenchyma can be used to quantify progression of emphysematous destruction. Stoeckley used the P15 to test the effect of intravenous α−1 antitrypsin against placebo and could quantify a relative reduction of emphysema progression in the pharmaceutical arm.[131]

Asthma severity: proximal and distal airway

The airway remodelling seen in asthmatic patients is a morphological feature that yields substantial promise of imaging biomarkers for personalized asthma care.[132,133] Airway remodelling is particularly targeted on QCT, notably, there is association between epithelial thickness and central airway quantification by CT.[94] This association led to definition of CT-based clinical clusters of asthma, with different clinical and therapeutic features. The imaging-based clustering of asthmatic patients was first proposed by Gupta, who found heterogeneity of response to bronchodilator in patients with different imaging cluster[92] (Figure 5). Recently, further description of asthma clusters has been obtained including topographic metrics of air trapping, with substantial clinical relevance compared to asthma phenotypes based on the sole clinical characterization or sputum cell count.[88] Noteworthy, Choi reported that the four imaging-based clusters show different response to high-dose inhaled corticosteroids.[88]

Longitudinal quantification of air trapping extent by CT has been used as biomarker to assess response to treatment,[134–136] furthermore, it was associated with vascular conspicuity in proximal airway wall.[94]

This evidence and its logarithmic technical development foster readily available quantitative metrics to assess personalized asthma care in clinical trials and potential translation to clinical use of imaging-based asthma phenotypes.

INTERSTITIAL LUNG DISEASE

The variability in clinical evaluation of ILD is a reason for automation, CAD, and quantitative image analysis.[137] Several studies showed that QCT is an objective analysis that may overcome the issue of the interobserver variability and could provide more consistent prognostic indexes.[138–142] Furthermore, QCT has the potential ability to identify CT features that are not visually recognizable and to objectively monitor the disease progression on serial CT scans.

State of the art

There are several quantitative CT systems of varying degrees of sophistication for the assessment of ILD. As opposed to pulmonary emphysema, ILD patterns are quite heterogeneous in morphologic characteristics and lack a standard density threshold that can dichotomize the visualized lung tissue into normal and diseased.[143] Nevertheless, the global histogram of density metrics of CT images—skewness, kurtosis and mean lung density—are helpful to estimate the ILD extent.[144–146] For instance, in pulmonary fibrosis, collagen deposition increases lung density, causing a rightward shift of the CT frequency histogram and reducing its peak (*i.e.* increasing skewness and kurtosis, respectively).[147] Furthermore, such metrics are sufficiently reproducible and not substantially affected by the reduction in radiation dose in subjects with ILD.[148–150]

Lung volume variation due to different levels of inspiration may represent a major limitation of any density-based analysis of the lungs. Such a noise may be attenuated by evaluating the lung weight, which takes into account both lung volume and lung density.[151]

QCT was reported to enable objective tracking of the changes in lung weight and air-space inflation produced by a standard intervention, as in pulmonary alveolar proteinosis, suggesting lung weight could be a reliable metric to assess longitudinal change in ILDs (*e.g.* diffuse acute lung disorders).[152] The density histogram parameters have also been used to quantify the extent of individual patterns of ILD (*e.g.* ground glass opacity, honeycombing, reticulation etc.).[153] This approach is not sufficient to achieve that goal, and more sophisticated textural analyses have been, therefore, implemented.[2] Parenchymal classification is applied to voxel volume unit (*e.g.* discrete volume that allows detailed characterization of local parenchymal features) using TA, computer

Figure 6. (a–j) Longitudinal quantitative analysis of fibrotic interstitial lung disease. Automatic volumetric segmentation of parenchymal abnormalities in a patient with idiopathic pulmonary fibrosis at baseline (top row: a–e) and 1-year follow-up (bottom row: f–j). The colour-coded overlay on native high resolution computed tomography (HRCT) images shows the distribution of parenchymal abnormalities on axial, coronal and sagittal reconstruction at baseline (a–c) and 1 year (f–h). The data are also provided in a volumetric model that shows both lungs with colour-coded characterization of parenchyma volume. Furthermore, a synthetic 2D graph (the so-called Glyph) is built that provides comprehensive display of abnormal parenchyma and its distribution between lobes (baseline Glyph in e, 1-year Glyph in j). 2D, two-dimensional.

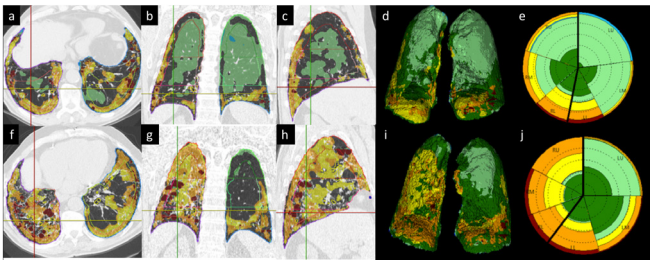

vision-based image understanding of volumetric histogram signature mapping features and three-dimensional-morphology. Textural analysis is based on ROIs selected by trained observers in the lung, according to a set of specific patterns (normal, reticular, honeycombing etc.) (Figure 6). The histogram or textural features of each volumetric ROI are extracted, and a machine-learning algorithm is used to develop a predictive model for specific patterns.[137,154–156] Given the well-known interobserver variability for the assessment of honeycombing, the development of an objective quantitative CT tool that can quantify honeycombing with prognostic value is of utmost importance. However, this kind of software analysis is limited by inbuilt subjectivity (*e.g.* owed to the expert observers pretraining), and other objective methods are currently being developed.[2,157]

Most textural-based software is still not commercially available on CT vendors' diagnostic workstations and such software requires high-resolution images, preferably reconstructed with parameters that reduce image noise. Such multidimensional analysis demands considerable computational power that usually requires a dedicated workstation outside of the clinical radiology workflow.[154]

There are still some important topics that need to be addressed in the future. First, it's not fully clear if (and to what extent) CT technique optimization and standardization should be pursued for the quantitative analysis of ILD. This may have important implications for multicentre clinical trials that rely on accurate and reproducible quantitative analysis of CT images collected under varied conditions across multiple sites, scanners and time points.[157] Second, most QCT metrics of ILD severity are given as continuous data and are not, therefore, user-friendly for clinical practice. A staging system that defines ILD severity in categories (*e.g.* mild, moderate or severe) would be helpful for implementing QCT in clinical practice.[138]

Application in scientific investigation and clinical trials

Most investigations have tested QCT tools in subjects with either idiopathic pulmonary fibrosis (IPF), or connective tissue disease (*e.g.* systemic sclerosis).[141,142,145,146,150,156,158] At present, automated image analysis of ILD is still confined to the research setting.

A large number of studies demonstrated that various QCT metrics correlated with several clinicofunctional indexes.[139,140,146,150,159,160] However, data on their prognostic value is of outmost importance. Best et al[161] showed both kurtosis and visual scoring of the extent of fibrosing pattern as the only predictors of mortality in a retrospective study of 167 subjects with IPF recruited in a clinical trial. Recently, in a study of 46 subjects with IPF the histogram metrics correlated with PFT and were associated with transplant free survival similarly to the visual scoring performed by two experts.[153] Likewise, the histogram metrics can discriminate between well-defined different mortality risk categories in subjects with systemic sclerosis-related ILD.[142]

Jacob showed that baseline texture-based CT quantification of total disease extent or individual patterns were superior to visual scoring in increasing the accuracy of clinicofunctional models predictive of outcome in IPF.[138] Intriguingly, the authors showed that the pulmonary vessels volume (PVV), was the individual QCT metric more strongly associated with mortality. Several hypotheses have been suggested, though the pathophysiological mechanism is not yet understood and further validation is required. Furthermore, they subsequently demonstrated that the PVV was also an independent predictor of mortality across patients with various connective tissue diseases.[162]

The visual scoring of serial CTs is not fully standardized and QCT analysis may be particularly attractive for objectively monitoring IPF.[2] Maldonado showed that short-term (3–15 months) changes in CT patterns as assessed by the software was predictive of survival.[141] Likewise, two recent studies using another software, showed that automatic quantification of lung fibrosis at CT yields an index of severity that correlates with visual assessment and functional change in subjects with IPF.[156,158]

However, the assessment of the severity of traction bronchiectasis—a major determinant of prognosis as visually quantified in subjects with either IPF or connective tissue disease—is still not allowed by any QCT tool.

CONCLUSION

There is a large amount of data that support the potential of QCT in pulmonary medicine. The fast technological development of such tools already brought to their clinical application, especially for the assessment of lung nodule and its management standardization. Furthermore, the prognostic yield of QCT in diffuse lung diseases is challenging the traditional approach based on clinical and functional assessment. Notably, QCT analysis has its strength in detailed volumetric characterization of lung parenchyma, and thus the potential

to apportion the contribution of single heterogeneous determinants of lung disease. This characteristic appears particularly useful for clinical trials and, potentially, for selection of personalized treatment.

The future of QCT is granted by the logarithmic technological development that suggests computerized medical systems will integrate automatic data analysis in clinical practice for multidisciplinary prognostication and management of patient with pulmonary disease.

ACKNOWLEDGMENTS

The authors thank Dr Sumit Gupta for the iconographic contribution.

REFERENCES

1. Goldin JG. Computed tomography as a biomarker in clinical trials imaging. *J Thorac Imaging* 2013; **28**: 291–7. doi: https://doi.org/10.1097/RTI.0b013e3182a1d93d
2. Hansell DM, Goldin JG, King TE, Lynch DA, Richeldi L, Wells AU. CT staging and monitoring of fibrotic interstitial lung diseases in clinical practice and treatment trials: a position paper from the Fleischner Society. *Lancet Respir Med* 2015; **3**: 483–96. doi: https://doi.org/10.1016/S2213-2600(15)00096-X
3. Al Mohammad B, Brennan PC, Mello-Thoms C. A review of lung cancer screening and the role of computer-aided detection. *Clin Radiol* 2017; **72**. doi: https://doi.org/10.1016/j.crad.2017.01.002
4. Labaki WW, Martinez CH, Martinez FJ, Galbán CJ, Ross BD, Washko GR, et al. The role of chest computed tomography in the evaluation and management of the patient with COPD. *Am J Respir Crit Care Med* 2017;. doi: https://doi.org/10.1164/rccm.201703-0451PP
5. Brown MS, Lo P, Goldin JG, Barnoy E, Kim GH, McNitt-Gray MF, et al. Toward clinically usable CAD for lung cancer screening with computed tomography. *Eur Radiol* 2014; **24**: 2719–28. doi: https://doi.org/10.1007/s00330-014-3329-0
6. van Klaveren RJ, Oudkerk M, Prokop M, Scholten ET, Nackaerts K, Vernhout R, et al. Management of lung nodules detected by volume CT scanning. *N Engl J Med* 2009; **361**: 2221–9. doi: https://doi.org/10.1056/NEJMoa0906085
7. Sverzellati N, Silva M, Calareso G, Galeone C, Marchianò A, Sestini S, et al. Low-dose computed tomography for lung cancer screening: comparison of performance between annual and biennial screen. *Eur Radiol* 2016; **26**: 3821–9. doi: https://doi.org/10.1007/s00330-016-4228-3
8. Becker N, Motsch E, Gross ML, Eigentopf A, Heussel CP, Dienemann H, et al. Randomized study on early detection of lung cancer with MSCT in Germany: results of the first 3 years of follow-up after randomization. *J Thorac Oncol* 2015; **10**: 890–6. doi: https://doi.org/10.1097/JTO.0000000000000530
9. Goo JM. A computer-aided diagnosis for evaluating lung nodules on chest CT: the current status and perspective. *Korean J Radiol* 2011; **12**: 145–55. doi: https://doi.org/10.3348/kjr.2011.12.2.145
10. Matsumoto S, Ohno Y, Aoki T, Yamagata H, Nogami M, Matsumoto K, et al. Computer-aided detection of lung nodules on multidetector CT in concurrent-reader and second-reader modes: a comparative study. *Eur J Radiol* 2013; **82**: 1332–7. doi: https://doi.org/10.1016/j.ejrad.2013.02.005
11. Beyer F, Zierott L, Fallenberg EM, Juergens KU, Stoeckel J, Heindel W, et al. Comparison of sensitivity and reading time for the use of computer-aided detection (CAD) of pulmonary nodules at MDCT as concurrent or second reader. *Eur Radiol* 2007; **17**: 2941–7. doi: https://doi.org/10.1007/s00330-007-0667-1
12. Martini K, Barth BK, Nguyen-Kim TD, Baumueller S, Alkadhi H, Frauenfelder T. Evaluation of pulmonary nodules and infection on chest CT with radiation dose equivalent to chest radiography: prospective intra-individual comparison study to standard dose CT. *Eur J Radiol* 2016; **85**: 360–5. doi: https://doi.org/10.1016/j.ejrad.2015.11.036
13. Messerli M, Kluckert T, Knitel M, Rengier F, Warschkow R, Alkadhi H, et al. Computer-aided detection (CAD) of solid pulmonary nodules in chest x-ray equivalent ultralow dose chest CT - first in-vivo results at dose levels of 0.13mSv. *Eur J Radiol* 2016; **85**: 2217–24. doi: https://doi.org/10.1016/j.ejrad.2016.10.006
14. Den Harder AM, Willemink MJ, van Hamersvelt RW, Vonken EJ, Milles J, Schilham AM, et al. Effect of radiation dose reduction and iterative reconstruction on computer-aided detection of pulmonary nodules: Intra-individual comparison. *Eur J Radiol* 2016; **85**: 346–51. doi: https://doi.org/10.1016/j.ejrad.2015.12.003
15. Christe A, Leidolt L, Huber A, Steiger P, Szucs-Farkas Z, Roos JE, et al. Lung cancer screening with CT: evaluation of radiologists and different computer assisted detection software (CAD) as first and second readers for lung nodule detection at different dose levels. *Eur J Radiol* 2013; **82**: e873–8. doi: https://doi.org/10.1016/j.ejrad.2013.08.026
16. Hein PA, Rogalla P, Klessen C, Lembcke A, Romano VC. Computer-aided pulmonary nodule detection - performance of two CAD systems at different CT dose levels. *Rofo* 2009; **181**: 1056–64. doi: https://doi.org/10.1055/s-0028-1109394
17. Jacobs C, van Rikxoort EM, Twellmann T, Scholten ET, de Jong PA, Kuhnigk JM, et al. Automatic detection of subsolid pulmonary nodules in thoracic computed tomography images. *Med Image Anal* 2014; **18**: 374–84. doi: https://doi.org/10.1016/j.media.2013.12.001
18. Wormanns D, Fiebich M, Saidi M, Diederich S, Heindel W. Automatic detection of pulmonary nodules at spiral CT: clinical application of a computer-aided diagnosis system. *Eur Radiol* 2002; **12**: 1052–7. doi: https://doi.org/10.1007/s003300101126
19. Armato SG. 3rd, Giger ML, Moran CJ, Blackburn JT, Doi K, MacMahon H. Computerized detection of pulmonary nodules on CT scans. *Radiographics* 1999; **19**: 1303–11.
20. Detterbeck FC, Bolejack V, Arenberg DA, Crowley J, Donington JS, Franklin WA, et al. The IASLC lung cancer staging project: background data and proposals for the classification of lung cancer with separate tumor nodules in the forthcoming eighth edition of the tnm classification for lung cancer. *J Thorac Oncol* 2016; **11**: 681–92. doi: https://doi.org/10.1016/j.jtho.2015.12.114
21. Zhao Y, de Bock GH, Vliegenthart R, van Klaveren RJ, Wang Y, Bogoni L, et al. Performance of computer-aided detection

of pulmonary nodules in low-dose CT: comparison with double reading by nodule volume. *Eur Radiol* 2012; **22**: 2076–84. doi: https://doi.org/10.1007/s00330-012-2437-y
22. Brown MS, Goldin JG, Suh RD, McNitt-Gray MF, Sayre JW, Aberle DR. Lung micronodules: automated method for detection at thin-section CT-initial experience. *Radiology* 2003; **226**: 256–62. doi: https://doi.org/10.1148/radiol.2261011708
23. Silva M, Pastorino U, Sverzellati N. Lung cancer screening with low-dose CT in Europe: strength and weakness of diverse independent screening trials. *Clin Radiol* 2017; **72**. doi: https://doi.org/10.1016/j.crad.2016.12.021
24. Benzakoun J, Bommart S, Coste J, Chassagnon G, Lederlin M, Boussouar S, et al. Computer-aided diagnosis (CAD) of subsolid nodules: evaluation of a commercial CAD system. *Eur J Radiol* 2016; **85**: 1728–34. doi: https://doi.org/10.1016/j.ejrad.2016.07.011
25. Godoy MC, Kim TJ, White CS, Bogoni L, de Groot P, Florin C, et al. Benefit of computer-aided detection analysis for the detection of subsolid and solid lung nodules on thin- and thick-section CT. *AJR Am J Roentgenol* 2013; **200**: 74–83. doi: https://doi.org/10.2214/AJR.11.7532
26. Silva M, Capretti G, Sverzellati N, Jacobs C, Ciompi F, van Ginneken B. eds. *Subsolid and part-solid nodules in lung cancer screening: comparison between visual and computer-aided detection*. Vienna, AT: European Congress of Radiology Insights into Imaging; 2017.
27. van Ginneken B, Schaefer-Prokop CM, Prokop M. Computer-aided diagnosis: how to move from the laboratory to the clinic. *Radiology* 2011; **261**: 719–32. doi: https://doi.org/10.1148/radiol.11091710
28. Henschke CI, Yankelevitz DF, Mirtcheva R, McGuinness G, McCauley D, Miettinen OS, et al. CT screening for lung cancer: frequency and significance of part-solid and nonsolid nodules. *AJR Am J Roentgenol* 2002; **178**: 1053–7. doi: https://doi.org/10.2214/ajr.178.5.1781053
29. Wilson R, Devaraj A. Radiomics of pulmonary nodules and lung cancer. *Transl Lung Cancer Res* 2017; **6**: 86–91. doi: https://doi.org/10.21037/tlcr.2017.01.04
30. Colombi D, Manna C, Montermini I, Seletti V, Diciotti S, Tiseo M, et al. Semiautomatic analysis on computed tomography in locally advanced or metastatic non-small cell lung cancer: reproducibility and prognostic significance of unidimensional and 3-dimensional measurements. *J Thorac Imaging* 2015; **30**: 290–9. doi: https://doi.org/10.1097/RTI.0000000000000145
31. Kim H, Park CM, Goo JM, Wildberger JE, Kauczor HU. Quantitative computed tomography imaging biomarkers in the diagnosis and management of lung cancer. *Invest Radiol* 2015; **50**: 571–83. doi: https://doi.org/10.1097/RLI.0000000000000152
32. Liang M, Yip R, Tang W, Xu D, Reeves A, Henschke CI, et al. Variation in screening CT-detected nodule volumetry as a function of size. *AJR Am J Roentgenol* 2017; **209**: 304–8. doi: https://doi.org/10.2214/AJR.16.17159
33. Moser JB, Mak SM, McNulty WH, Padley S, Nair A, Shah PL, et al. The influence of inspiratory effort and emphysema on pulmonary nodule volumetry reproducibility. *Clin Radiol* 2017; **72**: 925–9. doi: https://doi.org/10.1016/j.crad.2017.06.117
34. Xu DM, Gietema H, de Koning H, Vernhout R, Nackaerts K, Prokop M, et al. Nodule management protocol of the NELSON randomised lung cancer screening trial. *Lung Cancer* 2006; **54**: 177–84. doi: https://doi.org/10.1016/j.lungcan.2006.08.006
35. Marchianò A, Calabrò E, Civelli E, Di Tolla G, Frigerio LF, Morosi C, et al. Pulmonary nodules: volume repeatability at multidetector CT lung cancer screening. *Radiology* 2009; **251**: 919–25. doi: https://doi.org/10.1148/radiol.2513081313
36. de Hoop B, Gietema H, van de Vorst S, Murphy K, van Klaveren RJ, Prokop M. Pulmonary ground-glass nodules: increase in mass as an early indicator of growth. *Radiology* 2010; **255**: 199–206. doi: https://doi.org/10.1148/radiol.09090571
37. Mets OM, de Jong PA, Chung K, Lammers JJ, van Ginneken B, Schaefer-Prokop CM. Fleischner recommendations for the management of subsolid pulmonary nodules: high awareness but limited conformance - a survey study. *Eur Radiol* 2016; **26**. doi: https://doi.org/10.1007/s00330-016-4249-y
38. Zhao YR, van Ooijen PM, Dorrius MD, Heuvelmans M, de Bock GH, Vliegenthart R, et al. Comparison of three software systems for semi-automatic volumetry of pulmonary nodules on baseline and follow-up CT examinations. *Acta Radiol* 2014; **55**: 691–8. doi: https://doi.org/10.1177/0284185113508177
39. van Ginneken B. Fifty years of computer analysis in chest imaging: rule-based, machine learning, deep learning. *Radiol Phys Technol* 2017; **10**: 23–32. doi: https://doi.org/10.1007/s12194-017-0394-5
40. Castellino RA. Computer aided detection (CAD): an overview. *Cancer Imaging* 2005; **5**: 17–19. doi: https://doi.org/10.1102/1470-7330.2005.0018
41. Javaid M, Javid M, Rehman MZ, Shah SI. A novel approach to CAD system for the detection of lung nodules in CT images. *Comput Methods Programs Biomed* 2016; **135**: 125–39. doi: https://doi.org/10.1016/j.cmpb.2016.07.031
42. Das M, Mühlenbruch G, Mahnken AH, Flohr TG, Gündel L, Stanzel S, et al. Small pulmonary nodules: effect of two computer-aided detection systems on radiologist performance. *Radiology* 2006; **241**: 564–71. doi: https://doi.org/10.1148/radiol.2412051139
43. Jacobs C, van Rikxoort EM, Murphy K, Prokop M, Schaefer-Prokop CM, van Ginneken B. Computer-aided detection of pulmonary nodules: a comparative study using the public LIDC/IDRI database. *Eur Radiol* 2016; **26**: 2139–47. doi: https://doi.org/10.1007/s00330-015-4030-7
44. Lee JW, Goo JM, Lee HJ, Kim JH, Kim S, Kim YT. The potential contribution of a computer-aided detection system for lung nodule detection in multidetector row computed tomography. *Invest Radiol* 2004; **39**: 649–55.
45. Infante M, Sestini S, Galeone C, Marchiano A, Lutman FR, Angeli E. Lung cancer screening with low-dose spiral computed tomography: evidence from a pooled analysis of two Italian randomized trials. *Eur J Cancer Prev* 2016; **26**: 324–9.
46. Parekh V, Jacobs MA. Radiomics: a new application from established techniques. *Expert Rev Precis Med Drug Dev* 2016; **1**: 207–26. doi: https://doi.org/10.1080/23808993.2016.1164013
47. Erickson BJ, Korfiatis P, Akkus Z, Kline TL. Machine learning for medical imaging. *Radiographics* 2017; **37**: 505–15. doi: https://doi.org/10.1148/rg.2017160130
48. Larue RT, Defraene G, De Ruysscher D, Lambin P, van Elmpt W. Quantitative radiomics studies for tissue characterization: a review of technology and methodological procedures. *Br J Radiol* 2017; **90**: 20160665. doi: https://doi.org/10.1259/bjr.20160665
49. Lambin P, Rios-Velazquez E, Leijenaar R, Carvalho S, van Stiphout RG, Granton P, et al. Radiomics: extracting more information from medical images using advanced feature analysis. *Eur J Cancer* 2012; **48**: 441–6. doi: https://doi.org/10.1016/j.ejca.2011.11.036

50. Balagurunathan Y, Gu Y, Wang H, Kumar V, Grove O, Hawkins S, et al. Reproducibility and prognosis of quantitative features extracted from CT images. *Transl Oncol* 2014; **7**: 72–87.
51. Kim H, Park CM, Lee M, Park SJ, Song YS, Lee JH, et al. Impact of reconstruction algorithms on CT radiomic features of pulmonary tumors: analysis of intra- and inter-reader variability and inter-reconstruction algorithm variability. *PLoS One* 2016; **11**: e0164924. doi: https://doi.org/10.1371/journal.pone.0164924
52. Coroller TP, Grossmann P, Hou Y, Rios Velazquez E, Leijenaar RT, Hermann G, et al. CT-based radiomic signature predicts distant metastasis in lung adenocarcinoma. *Radiother Oncol* 2015; **114**: 345–50. doi: https://doi.org/10.1016/j.radonc.2015.02.015
53. Mackin D, Fave X, Zhang L, Fried D, Yang J, Taylor B, et al. Measuring computed tomography scanner variability of radiomics features. *Invest Radiol* 2015; **50**: 757–65. doi: https://doi.org/10.1097/RLI.0000000000000180
54. Solomon J, Mileto A, Nelson RC, Roy Choudhury K, Samei E. Quantitative features of liver lesions, lung nodules, and renal stones at multi-detector row CT examinations: dependency on radiation dose and reconstruction algorithm. *Radiology* 2016; **279**: 185–94. doi: https://doi.org/10.1148/radiol.2015150892
55. Hawkins S, Wang H, Liu Y, Garcia A, Stringfield O, Krewer H, et al. Predicting malignant nodules from screening CT scans. *J Thorac Oncol* 2016; **11**: 2120–8. doi: https://doi.org/10.1016/j.jtho.2016.07.002
56. Lee SH, Lee SM, Goo JM, Kim KG, Kim YJ, Park CM. Usefulness of texture analysis in differentiating transient from persistent part-solid nodules (PSNs): a retrospective study. *PLoS One* 2014; **9**: e85167. doi: https://doi.org/10.1371/journal.pone.0085167
57. Chae HD, Park CM, Park SJ, Lee SM, Kim KG, Goo JM. Computerized texture analysis of persistent part-solid ground-glass nodules: differentiation of preinvasive lesions from invasive pulmonary adenocarcinomas. *Radiology* 2014; **273**: 285–93. doi: https://doi.org/10.1148/radiol.14132187
58. Nemec U, Heidinger BH, Anderson KR, Westmore MS, VanderLaan PA, Bankier AA. Software-based risk stratification of pulmonary adenocarcinomas manifesting as pure ground glass nodules on computed tomography. *Eur Radiol* 2017;. doi: https://doi.org/10.1007/s00330-017-4937-2
59. Choi ER, Lee HY, Jeong JY, Choi YL, Kim J, Bae J, et al. Quantitative image variables reflect the intratumoral pathologic heterogeneity of lung adenocarcinoma. *Oncotarget* 2016; **7**: 67302–13. doi: https://doi.org/10.18632/oncotarget.11693
60. Gillies RJ, Kinahan PE, Hricak H. Radiomics: images are more than pictures, they are data. *Radiology* 2016; **278**: 563–77. doi: https://doi.org/10.1148/radiol.2015151169
61. Ganeshan B, Miles KA. Quantifying tumour heterogeneity with CT. *Cancer Imaging* 2013; **13**: 140–9. doi: https://doi.org/10.1102/1470-7330.2013.0015
62. Mattonen SA, Huang K, Ward AD, Senan S, Palma DA. New techniques for assessing response after hypofractionated radiotherapy for lung cancer. *J Thorac Dis* 2014; **6**: 375–86. doi: https://doi.org/10.3978/j.issn.2072-1439.2013.11.09
63. Ravanelli M, Farina D, Morassi M, Roca E, Cavalleri G, Tassi G, et al. Texture analysis of advanced non-small cell lung cancer (NSCLC) on contrast-enhanced computed tomography: prediction of the response to the first-line chemotherapy. *Eur Radiol* 2013; **23**: 3450–5. doi: https://doi.org/10.1007/s00330-013-2965-0
64. Aerts HJ, Velazquez ER, Leijenaar RT, Parmar C, Grossmann P, Carvalho S, et al. Decoding tumour phenotype by noninvasive imaging using a quantitative radiomics approach. *Nat Commun* 2014; **5**: 4006. doi: https://doi.org/10.1038/ncomms5006
65. Ahn SY, Park CM, Park SJ, Kim HJ, Song C, Lee SM, et al. Prognostic value of computed tomography texture features in non-small cell lung cancers treated with definitive concomitant chemoradiotherapy. *Invest Radiol* 2015; **50**: 719–25. doi: https://doi.org/10.1097/RLI.0000000000000174
66. Ganeshan B, Panayiotou E, Burnand K, Dizdarevic S, Miles K. Tumour heterogeneity in non-small cell lung carcinoma assessed by CT texture analysis: a potential marker of survival. *Eur Radiol* 2012; **22**: 796–802. doi: https://doi.org/10.1007/s00330-011-2319-8
67. Parmar C, Leijenaar RT, Grossmann P, Rios Velazquez E, Bussink J, Rietveld D, et al. Radiomic feature clusters and prognostic signatures specific for Lung and Head & Neck cancer. *Sci Rep* 2015; **5**: 11044. doi: https://doi.org/10.1038/srep11044
68. Coxson HO, Leipsic J, Parraga G, Sin DD. Using pulmonary imaging to move chronic obstructive pulmonary disease beyond FEV1. *Am J Respir Crit Care Med* 2014; **190**: 135–44. doi: https://doi.org/10.1164/rccm.201402-0256PP
69. Tseng HJ, Henry TS, Veeraraghavan S, Mittal PK, Little BP. Pulmonary function tests for the radiologist. *Radiographics* 2017; **37**: 1037–58. doi: https://doi.org/10.1148/rg.2017160174
70. Milanese G, Silva M, Sverzellati N. Lung volume reduction of pulmonary emphysema: the radiologist task. *Curr Opin Pulm Med* 2016; **22**: 179–86. doi: https://doi.org/10.1097/MCP.0000000000000252
71. Grenier PA, Fetita CI, Brillet PY. Quantitative computed tomography imaging of airway remodeling in severe asthma. *Quant Imaging Med Surg* 2016; **6**: 76–83. doi: https://doi.org/10.3978/j.issn.2223-4292.2016.02.08
72. Belloli EA, Degtiar I, Wang X, Yanik GA, Stuckey LJ, Verleden SE, et al. Parametric response mapping as an imaging biomarker in lung transplant recipients. *Am J Respir Crit Care Med* 2017; **195**: 942–52. doi: https://doi.org/10.1164/rccm.201604-0732OC
73. van Mastrigt E, Kakar E, Ciet P, den Dekker HT, Joosten KF, Kalkman P, et al. Structural and functional ventilatory impairment in infants with severe bronchopulmonary dysplasia. *Pediatr Pulmonol* 2017; **52**: 1029–37. doi: https://doi.org/10.1002/ppul.23696
74. Ciet P, Serra G, Bertolo S, Spronk S, Ros M, Fraioli F, et al. Assessment of CF lung disease using motion corrected PROPELLER MRI: a comparison with CT. *Eur Radiol* 2016; **26**: 780–7. doi: https://doi.org/10.1007/s00330-015-3850-9
75. Litmanovich DE, Hartwick K, Silva M, Bankier AA. Multidetector computed tomographic imaging in chronic obstructive pulmonary disease: emphysema and airways assessment. *Radiol Clin North Am* 2014; **52**: 137–54. doi: https://doi.org/10.1016/j.rcl.2013.09.002
76. Hoff BA, Pompe E, Galbán S, Postma DS, Lammers JJ, Ten Hacken NHT, et al. CT-Based local distribution metric improves characterization of COPD. *Sci Rep* 2017; **7**: 2999. doi: https://doi.org/10.1038/s41598-017-02871-1
77. Madani A, Van Muylem A, Gevenois PA. Pulmonary emphysema: effect of lung volume on objective quantification at thin-section CT. *Radiology* 2010; **257**: 260–8. doi: https://doi.org/10.1148/radiol.10091446
78. Bankier AA, De Maertelaer V, Keyzer C, Gevenois PA. Pulmonary emphysema: subjective visual grading versus objective quantification with macroscopic morphometry and thin-section CT

densitometry. *Radiology* 1999; **211**: 851–8. doi: https://doi.org/10.1148/radiology.211.3.r99jn05851

79. Mohamed Hoesein FA, de Hoop B, Zanen P, Gietema H, Kruitwagen CL, van Ginneken B, et al. CT-quantified emphysema in male heavy smokers: association with lung function decline. *Thorax* 2011; **66**: 782–7. doi: https://doi.org/10.1136/thx.2010.145995
80. Zach JA, Williams A, Jou SS, Yagihashi K, Everett D, Hokanson JE, et al. Current smoking status is associated with lower quantitative CT measures of emphysema and gas trapping. *J Thorac Imaging* 2016; **31**: 29–36. doi: https://doi.org/10.1097/RTI.0000000000000181
81. Washko GR, Kinney GL, Ross JC, San José Estépar R, Han MK, Dransfield MT, et al. Lung mass in smokers. *Acad Radiol* 2017; **24**: 386–92. doi: https://doi.org/10.1016/j.acra.2016.10.011
82. Schroeder JD, McKenzie AS, Zach JA, Wilson CG, Curran-Everett D, Stinson DS, et al. Relationships between airflow obstruction and quantitative CT measurements of emphysema, air trapping, and airways in subjects with and without chronic obstructive pulmonary disease. *AJR Am J Roentgenol* 2013; **201**: W460–70. doi: https://doi.org/10.2214/AJR.12.10102
83. Nambu A, Zach J, Schroeder J, Jin G, Kim SS, Kim YI, et al. Quantitative computed tomography measurements to evaluate airway disease in chronic obstructive pulmonary disease: relationship to physiological measurements, clinical index and visual assessment of airway disease. *Eur J Radiol* 2016; **85**: 2144–51. doi: https://doi.org/10.1016/j.ejrad.2016.09.010
84. Mohamed Hoesein FA, de Jong PA. Air trapping on computed tomography: regional versus diffuse. *Eur Respir J* 2017; **49**. doi: https://doi.org/10.1183/13993003.01791-2016
85. Galbán CJ, Han MK, Boes JL, Chughtai KA, Meyer CR, Johnson TD, et al. Computed tomography-based biomarker provides unique signature for diagnosis of COPD phenotypes and disease progression. *Nat Med* 2012; **18**: 1711–5. doi: https://doi.org/10.1038/nm.2971
86. Bodduluri S, Bhatt SP, Hoffman EA, Newell JD, Martinez CH, Dransfield MT, et al. Biomechanical CT metrics are associated with patient outcomes in COPD. *Thorax* 2017; **72**: 409–14. doi: https://doi.org/10.1136/thoraxjnl-2016-209544
87. Silva M, Nemec SF, Dufresne V, Occhipinti M, Heidinger BH, Chamberlain R, et al. Normal spectrum of pulmonary parametric response map to differentiate lung collapsibility: distribution of densitometric classifications in healthy adult volunteers. *Eur Radiol* 2016; **26**. doi: https://doi.org/10.1007/s00330-015-4133-1
88. Choi S, Hoffman EA, Wenzel SE, Castro M, Fain S, Jarjour N, et al. Quantitative computed tomographic imaging-based clustering differentiates asthmatic subgroups with distinctive clinical phenotypes. *J Allergy Clin Immunol* 2017; **140**. doi: https://doi.org/10.1016/j.jaci.2016.11.053
89. Charbonnier JP, Rikxoort EM, Setio AA, Schaefer-Prokop CM, Ginneken BV, Ciompi F. Improving airway segmentation in computed tomography using leak detection with convolutional networks. *Med Image Anal* 2017; **36**: 52–60. doi: https://doi.org/10.1016/j.media.2016.11.001
90. Koyama H, Ohno Y, Nishio M, Takenaka D, Yoshikawa T, Matsumoto S, et al. Three-dimensional airway lumen volumetry: comparison with bronchial wall area and parenchymal densitometry in assessment of airway obstruction in pulmonary emphysema. *Br J Radiol* 2012; **85**: 1525–32. doi: https://doi.org/10.1259/bjr/22602417
91. Hackx M, Francotte D, Garcia TS, Van Muylem A, Walsdorff M, Gevenois PA. Effect of total lung capacity, gender and height on CT airway measurements. *Br J Radiol* 2017; **90**: 20160898. doi: https://doi.org/10.1259/bjr.20160898
92. Gupta S, Hartley R, Khan UT, Singapuri A, Hargadon B, Monteiro W, et al. Quantitative computed tomography-derived clusters: redefining airway remodeling in asthmatic patients. *J Allergy Clin Immunol* 2014; **13338**: 729–38. doi: https://doi.org/10.1016/j.jaci.2013.09.039
93. Leutz-Schmidt P, Weinheimer O, Jobst BJ, Dinkel J, Biederer J, Kauczor HU, et al. Influence of exposure parameters and iterative reconstruction on automatic airway segmentation and analysis on MDCT-An ex vivo phantom study. *PLoS One* 2017; **12**: e0182268. doi: https://doi.org/10.1371/journal.pone.0182268
94. Berair R, Hartley R, Mistry V, Sheshadri A, Gupta S, Singapuri A, et al. Associations in asthma between quantitative computed tomography and bronchial biopsy-derived airway remodelling. *Eur Respir J* 2017; **49**. doi: https://doi.org/10.1183/13993003.01507-2016
95. Crisafulli E, Alfieri V, Silva M, Aiello M, Tzani P, Milanese G, et al. Relationships between emphysema and airways metrics at high-resolution computed tomography (HRCT) and ventilatory response to exercise in mild to moderate COPD patients. *Respir Med* 2016; **117**: 207–14. doi: https://doi.org/10.1016/j.rmed.2016.06.016
96. Ash SY, Diaz AA. The role of imaging in the assessment of severe asthma. *Curr Opin Pulm Med* 2017; **23**: 97–102. doi: https://doi.org/10.1097/MCP.0000000000000341
97. Brillet PY, Fetita CI, Capderou A, Mitrea M, Dreuil S, Simon JM, et al. Variability of bronchial measurements obtained by sequential CT using two computer-based methods. *Eur Radiol* 2009; **19**: 1139–47. doi: https://doi.org/10.1007/s00330-008-1247-8
98. Hackx M, Gyssels E, Severo Garcia T, De Meulder I, Alard S, Bruyneel M, et al. Chronic obstructive pulmonary disease: CT quantification of airway dimensions, numbers of airways to measure, and effect of bronchodilation. *Radiology* 2015; **277**: 853–62. doi: https://doi.org/10.1148/radiol.2015140949
99. Lederlin M, Laurent F, Portron Y, Ozier A, Cochet H, Berger P, et al. CT attenuation of the bronchial wall in patients with asthma: comparison with geometric parameters and correlation with function and histologic characteristics. *AJR Am J Roentgenol* 2012; **199**: 1226–33. doi: https://doi.org/10.2214/AJR.11.8396
100. Shim SS, Schiebler ML, Sorkness RL, Jarjour N, Kanne JP, Fain SB. *Post-processing of 3rd and 4th generation bronchial luminal cross-sectional area at end-expiration significantly differs in asthmatics: a newly discovered biomechanical difference found in Severe Asthma Research Program (SARP) subjects. Radiological Society of North America 2014 Scientific Assembly and Annual Meeting.* Chicago IL; 2014.
101. Diaz AA, Young TP, Maselli DJ, Martinez CH, Gill R, Nardelli P, et al. Quantitative CT measures of bronchiectasis in smokers. *Chest* 2017; **151**: 1255–62. doi: https://doi.org/10.1016/j.chest.2016.11.024
102. Estépar RS, Kinney GL, Black-Shinn JL, Bowler RP, Kindlmann GL, Ross JC, et al. Computed tomographic measures of pulmonary vascular morphology in smokers and their clinical implications. *Am J Respir Crit Care Med* 2013; **188**: 231–9. doi: https://doi.org/10.1164/rccm.201301-0162OC
103. Iyer KS, Newell JD, Jin D, Fuld MK, Saha PK, Hansdottir S, et al. Quantitative dual-energy computed tomography supports a vascular etiology of smoking-induced inflammatory lung disease. *Am J Respir Crit Care Med* 2016; **193**: 652–61.

doi: https://doi.org/10.1164/rccm.201506-1196OC
104. Zhang LJ, Yang GF, Zhao YE, Zhou CS, Lu GM. Detection of pulmonary embolism using dual-energy computed tomography and correlation with cardiovascular measurements: a preliminary study. *Acta Radiol* 2009; **50**: 892–901. doi: https://doi.org/10.1080/02841850903095393
105. Goo HW, Goo JM. Dual-energy CT: new horizon in medical imaging. *Korean J Radiol* 2017; **18**: 555–69. doi: https://doi.org/10.3348/kjr.2017.18.4.555
106. Felloni P, Duhamel A, Faivre JB, Giordano J, Khung S, Deken V, et al. Regional distribution of pulmonary blood volume with dual-energy computed tomography: results in 42 subjects. *Acad Radiol* 2017; **24**: 1412–21. doi: https://doi.org/10.1016/j.acra.2017.05.003
107. Barr RG, Bluemke DA, Ahmed FS, Carr JJ, Enright PL, Hoffman EA, et al. Percent emphysema, airflow obstruction, and impaired left ventricular filling. *N Engl J Med* 2010; **362**: 217–27. doi: https://doi.org/10.1056/NEJMoa0808836
108. Sieren JP, Newell JD, Barr RG, Bleecker ER, Burnette N, Carretta EE, et al. SPIROMICS protocol for multicenter quantitative computed tomography to phenotype the lungs. *Am J Respir Crit Care Med* 2016; **194**: 794–806. doi: https://doi.org/10.1164/rccm.201506-1208PP
109. (QIBA). QIBA. Available from: http://qibawiki.rsna.org/index.php/CT_Volumetry_Biomarker_Ctte [Accessed on August 10, 2017]
110. Chen-Mayer HH, Fuld MK, Hoppel B, Judy PF, Sieren JP, Guo J, et al. Standardizing CT lung density measure across scanner manufacturers. *Med Phys* 2017; **44**: 974–85. doi: https://doi.org/10.1002/mp.12087
111. Mets OM, Willemink MJ, de Kort FP, Mol CP, Leiner T, Oudkerk M, et al. The effect of iterative reconstruction on computed tomography assessment of emphysema, air trapping and airway dimensions. *Eur Radiol* 2012; **22**: 2103–9. doi: https://doi.org/10.1007/s00330-012-2489-z
112. Rodriguez A, Ranallo FN, Judy PF, Fain SB. The effects of iterative reconstruction and kernel selection on quantitative computed tomography measures of lung density. *Med Phys* 2017; **44**: 2267–80. doi: https://doi.org/10.1002/mp.12255
113. Theilig D, Doellinger F, Poellinger A, Schreiter V, Neumann K, Hubner RH. Comparison of distinctive models for calculating an interlobar emphysema heterogeneity index in patients prior to endoscopic lung volume reduction. *Int J Chron Obstruct Pulmon Dis* 2017; **12**: 1631–40. doi: https://doi.org/10.2147/COPD.S133348
114. Herth FJ, Noppen M, Valipour A, Leroy S, Vergnon JM, Ficker JH, et al. Efficacy predictors of lung volume reduction with Zephyr valves in a European cohort. *Eur Respir J* 2012; **39**: 1334–42. doi: https://doi.org/10.1183/09031936.00161611
115. Sverzellati N, Chetta A, Calabrò E, Carbognani P, Internullo E, Olivieri D, et al. Reliability of quantitative computed tomography to predict postoperative lung function in patients with chronic obstructive pulmonary disease having a lobectomy. *J Comput Assist Tomogr* 2005; **29**: 819–24. doi: https://doi.org/10.1097/01.rct.0000179595.09092.ee
116. Chandra D, Lipson DA, Hoffman EA, Hansen-Flaschen J, Sciurba FC, Decamp MM, et al. Perfusion scintigraphy and patient selection for lung volume reduction surgery. *Am J Respir Crit Care Med* 2010; **182**: 937–46. doi: https://doi.org/10.1164/rccm.201001-0043OC
117. Lynch DA, Al-Qaisi MA. Quantitative computed tomography in chronic obstructive pulmonary disease. *J Thorac Imaging* 2013; **28**: 284–90. doi: https://doi.org/10.1097/RTI.0b013e318298733c
118. Subramanian DR, Gupta S, Burggraf D, Vom Silberberg SJ, Heimbeck I, Heiss-Neumann MS, et al. Emphysema- and airway-dominant COPD phenotypes defined by standardised quantitative computed tomography. *Eur Respir J* 2016; **48**: 92–103. doi: https://doi.org/10.1183/13993003.01878-2015
119. Lynch DA, Austin JH, Hogg JC, Grenier PA, Kauczor HU, Bankier AA, et al. CT-definable subtypes of chronic obstructive pulmonary disease: a statement of the fleischner society. *Radiology* 2015; **277**: 192–205. doi: https://doi.org/10.1148/radiol.2015141579
120. Bhatt SP, Soler X, Wang X, Murray S, Anzueto AR, Beaty TH, et al. Association between functional small airway disease and fev1 decline in chronic obstructive pulmonary disease. *Am J Respir Crit Care Med* 2016; **194**: 178–84. doi: https://doi.org/10.1164/rccm.201511-2219OC
121. Boes JL, Hoff BA, Bule M, Johnson TD, Rehemtulla A, Chamberlain R, et al. Parametric response mapping monitors temporal changes on lung CT scans in the subpopulations and intermediate outcome measures in COPD Study (SPIROMICS. *Acad Radiol* 2015; **22**: 186–94. doi: https://doi.org/10.1016/j.acra.2014.08.015
122. Galbán CJ, Boes JL, Bule M, Kitko CL, Couriel DR, Johnson TD, et al. Parametric response mapping as an indicator of bronchiolitis obliterans syndrome after hematopoietic stem cell transplantation. *Biol Blood Marrow Transplant* 2014; **20**: 1592–8. doi: https://doi.org/10.1016/j.bbmt.2014.06.014
123. Regan EA, Hokanson JE, Murphy JR, Make B, Lynch DA, Beaty TH, et al. Genetic epidemiology of COPD (COPD Gene) study design. *COPD* 2010; **7**: 32–43. doi: https://doi.org/10.3109/15412550903499522
124. Agusti A, Calverley PM, Celli B, Coxson HO, Edwards LD, Lomas DA, et al. Characterisation of COPD heterogeneity in the ECLIPSE cohort. *Respir Res* 2010; **11**: 122. doi: https://doi.org/10.1186/1465-9921-11-122
125. Couper D, LaVange LM, Han M, Barr RG, Bleecker E, Hoffman EA, et al. Design of the subpopulations and intermediate outcomes in COPD study (SPIROMICS). *Thorax* 2014; **69**: 492–45. doi: https://doi.org/10.1136/thoraxjnl-2013-203897
126. Vestbo J, Agusti A, Wouters EF, Bakke P, Calverley PM, Celli B, et al. Should we view chronic obstructive pulmonary disease differently after ECLIPSE? A clinical perspective from the study team. *Am J Respir Crit Care Med* 2014; **189**: 1022–30. doi: https://doi.org/10.1164/rccm.201311-2006PP
127. Han MK, Quibrera PM, Carretta EE, Barr RG, Bleecker ER, Bowler RP, et al. Frequency of exacerbations in patients with chronic obstructive pulmonary disease: an analysis of the SPIROMICS cohort. *Lancet Respir Med* 2017; **5**: 619–26. doi: https://doi.org/10.1016/S2213-2600(17)30207-2
128. Han MK, Kazerooni EA, Lynch DA, Liu LX, Murray S, Curtis JL, et al. Chronic obstructive pulmonary disease exacerbations in the COPDGene study: associated radiologic phenotypes. *Radiology* 2011; **261**: 274–82. doi: https://doi.org/10.1148/radiol.11110173
129. Rahaghi FN, Vegas-Sanchez-Ferrero G, Minhas JK, Come CE, De La Bruere I, Wells JM, et al. Ventricular geometry from non-contrast non-ECG-gated CT scans: an imaging marker of cardiopulmonary disease in smokers. *Acad Radiol* 2017; **24**: 594–602. doi: https://doi.org/10.1016/j.acra.2016.12.007
130. Bhatt SP, Bodduluri S, Newell JD, Hoffman EA, Sieren JC, Han MK, et al. CT-derived biomechanical metrics improve

agreement between spirometry and emphysema. *Acad Radiol* 2016; **23**: 1255–63. doi: https://doi.org/10.1016/j.acra.2016.02.002

131. Stockley RA, Parr DG, Piitulainen E, Stolk J, Stoel BC, Dirksen A. Therapeutic efficacy of α-1 antitrypsin augmentation therapy on the loss of lung tissue: an integrated analysis of 2 randomised clinical trials using computed tomography densitometry. *Respir Res* 2010; **11**: 136. doi: https://doi.org/10.1186/1465-9921-11-136
132. Hartley R, Baldi S, Brightling C, Gupta S. Novel imaging approaches in adult asthma and their clinical potential. *Expert Rev Clin Immunol* 2015; **11**: 1147–62. doi: https://doi.org/10.1586/1744666X.2015.1072049
133. Brillet PY, Grenier PA, Fetita CI, Beigelman-Aubry C, Ould-Hmeidi Y, Ortner M, et al. Relationship between the airway wall area and asthma control score in moderate persistent asthma. *Eur Radiol* 2013; **23**: 1594–602. doi: https://doi.org/10.1007/s00330-012-2743-4
134. Tunon-de-Lara JM, Laurent F, Giraud V, Perez T, Aguilaniu B, Meziane H, et al. Air trapping in mild and moderate asthma: effect of inhaled corticosteroids. *J Allergy Clin Immunol* 2007; **119**: 583–90. doi: https://doi.org/10.1016/j.jaci.2006.11.005
135. Zeidler MR, Kleerup EC, Goldin JG, Kim HJ, Truong DA, Simmons MD, et al. Montelukast improves regional air-trapping due to small airways obstruction in asthma. *Eur Respir J* 2006; **27**: 307–15. doi: https://doi.org/10.1183/09031936.06.00005605
136. Haldar P, Brightling CE, Hargadon B, Gupta S, Monteiro W, Sousa A, et al. Mepolizumab and exacerbations of refractory eosinophilic asthma. *N Engl J Med* 2009; **360**: 973–84. doi: https://doi.org/10.1056/NEJMoa0808991
137. Bartholmai BJ, Raghunath S, Karwoski RA, Moua T, Rajagopalan S, Maldonado F, et al. Quantitative computed tomography imaging of interstitial lung diseases. *J Thorac Imaging* 2013; **28**: 298–307. doi: https://doi.org/10.1097/RTI.0b013e3182a21969
138. Jacob J, Bartholmai BJ, Rajagopalan S, Kokosi M, Nair A, Karwoski R, et al. Mortality prediction in idiopathic pulmonary fibrosis: evaluation of computer-based CT analysis with conventional severity measures. *Eur Respir J* 2017; **49**: 1601011. doi: https://doi.org/10.1183/13993003.01011-2016
139. Shin KE, Chung MJ, Jung MP, Choe BK, Lee KS. Quantitative computed tomographic indexes in diffuse interstitial lung disease: correlation with physiologic tests and computed tomography visual scores. *J Comput Assist Tomogr* 2011; **35**: 266–71. doi: https://doi.org/10.1097/RCT.0b013e31820ccf18
140. Park HJ, Lee SM, Song JW, Lee SM, Oh SY, Kim N, et al. Texture-based automated quantitative assessment of regional patterns on initial CT in patients with idiopathic pulmonary fibrosis: relationship to decline in forced vital capacity. *AJR Am J Roentgenol* 2016; **207**: 976–83. doi: https://doi.org/10.2214/AJR.16.16054
141. Maldonado F, Moua T, Rajagopalan S, Karwoski RA, Raghunath S, Decker PA, et al. Automated quantification of radiological patterns predicts survival in idiopathic pulmonary fibrosis. *Eur Respir J* 2014; **43**: 204–12. doi: https://doi.org/10.1183/09031936.00071812
142. Ariani A, Silva M, Seletti V, Bravi E, Saracco M, Parisi S, et al. Quantitative chest computed tomography is associated with two prediction models of mortality in interstitial lung disease related to systemic sclerosis. *Rheumatology* 2017; **56**: 922–7. doi: https://doi.org/10.1093/rheumatology/kew480
143. Sverzellati N, Calabrò E, Chetta A, Concari G, Larici AR, Mereu M, et al. Visual score and quantitative CT indices in pulmonary fibrosis: relationship with physiologic impairment. *Radiol Med* 2007; **112**: 1160–72. doi: https://doi.org/10.1007/s11547-007-0213-x
144. Hartley PG, Galvin JR, Hunninghake GW, Merchant JA, Yagla SJ, Speakman SB, et al. High-resolution CT-derived measures of lung density are valid indexes of interstitial lung disease. *J Appl Physiol* 1994; **76**: 271–7. doi: https://doi.org/(1985)
145. Best AC, Lynch AM, Bozic CM, Miller D, Grunwald GK, Lynch DA. Quantitative CT indexes in idiopathic pulmonary fibrosis: relationship with physiologic impairment. *Radiology* 2003; **228**: 407–14. doi: https://doi.org/10.1148/radiol.2282020274
146. Camiciottoli G, Orlandi I, Bartolucci M, Meoni E, Nacci F, Diciotti S, et al. Lung CT densitometry in systemic sclerosis: correlation with lung function, exercise testing, and quality of life. *Chest* 2007; **131**: 672–81. doi: https://doi.org/10.1378/chest.06-1401
147. Walsh SL, Nair A, Hansell DM. Post-processing applications in thoracic computed tomography. *Clin Radiol* 2013; **68**: 433–48. doi: https://doi.org/10.1016/j.crad.2012.05.018
148. Sverzellati N, Zompatori M, De Luca G, Chetta A, Bnà C, Ormitti F, et al. Evaluation of quantitative CT indexes in idiopathic interstitial pneumonitis using a low-dose technique. *Eur J Radiol* 2005; **56**: 370–5. doi: https://doi.org/10.1016/j.ejrad.2005.05.012
149. Iwasawa T, Kanauchi T, Hoshi T, Ogura T, Baba T, Gotoh T, et al. Multicenter study of quantitative computed tomography analysis using a computer-aided three-dimensional system in patients with idiopathic pulmonary fibrosis. *Jpn J Radiol* 2016; **34**: 16–27. doi: https://doi.org/10.1007/s11604-015-0496-0
150. Marten K, Dicken V, Kneitz C, Höhmann M, Kenn W, Hahn D, et al. Interstitial lung disease associated with collagen vascular disorders: disease quantification using a computer-aided diagnosis tool. *Eur Radiol* 2009; **19**: 324–32. doi: https://doi.org/10.1007/s00330-008-1152-1
151. Sverzellati N, Kuhnigk JM, Furia S, Diciotti S, Scanagatta P, Marchianò A, et al. CT-based weight assessment of lung lobes: comparison with ex vivo measurements. *Diagn Interv Radiol* 2013; **19**: 355–9. doi: https://doi.org/10.5152/dir.2013.149
152. Perez A, Coxson HO, Hogg JC, Gibson K, Thompson PF, Rogers RM. Use of CT morphometry to detect changes in lung weight and gas volume. *Chest* 2005; **128**: 2471–7. doi: https://doi.org/10.1378/chest.128.4.2471
153. Ash SY, Harmouche R, Vallejo DL, Villalba JA, Ostridge K, Gunville R, et al. Densitometric and local histogram based analysis of computed tomography images in patients with idiopathic pulmonary fibrosis. *Respir Res* 2017; **18**: 45. doi: https://doi.org/10.1186/s12931-017-0527-8
154. Sverzellati N, Brillet PY. When deep blue first defeated Kasparov: is a machine stronger than a radiologist at predicting prognosis in idiopathic pulmonary fibrosis? *Eur Respir J* 2017; **49**: 1602144. doi: https://doi.org/10.1183/13993003.02144-2016
155. Uppaluri R, Hoffman EA, Sonka M, Hunninghake GW, McLennan G. Interstitial lung disease: a quantitative study using the adaptive multiple feature method. *Am J Respir Crit Care Med* 1999; **159**: 519–25. doi: https://doi.org/10.1164/ajrccm.159.2.9707145
156. Salisbury ML, Lynch DA, van Beek EJ, Kazerooni EA, Guo J, Xia M, et al. Idiopathic pulmonary fibrosis: the association between the adaptive multiple features method and fibrosis outcomes. *Am J Respir Crit Care Med* 2017; **195**: 921–9. doi: https://doi.org/10.1164/rccm.201607-1385OC

157. Chong DY, Kim HJ, Lo P, Young S, McNitt-Gray MF, Abtin F, et al. Robustness-driven feature selection in classification of fibrotic interstitial lung disease patterns in computed tomography using 3D texture features. *IEEE Trans Med Imaging* 2016; **35**: 144–57. doi: https://doi.org/10.1109/TMI.2015.2459064
158. Humphries SM, Yagihashi K, Huckleberry J, Rho BH, Schroeder JD, Strand M, et al. Idiopathic pulmonary fibrosis: data-driven textural analysis of extent of fibrosis at baseline and 15-month follow-up. *Radiology* 2017; **161177285**: 270–8. doi: https://doi.org/10.1148/radiol.2017161177
159. Jacob J, Bartholmai BJ, Rajagopalan S, Kokosi M, Nair A, Karwoski R, et al. Automated quantitative computed tomography versus visual computed tomography scoring in idiopathic pulmonary fibrosis: validation against pulmonary function. *J Thorac Imaging* 2016; **31**: 304–11. doi: https://doi.org/10.1097/RTI.0000000000000220
160. Khanna D, Nagaraja V, Tseng CH, Abtin F, Suh R, Kim G, et al. Predictors of lung function decline in scleroderma-related interstitial lung disease based on high-resolution computed tomography: implications for cohort enrichment in systemic sclerosis-associated interstitial lung disease trials. *Arthritis Res Ther* 2015; **17**: 372. doi: https://doi.org/10.1186/s13075-015-0872-2
161. Best AC, Meng J, Lynch AM, Bozic CM, Miller D, Grunwald GK, et al. Idiopathic pulmonary fibrosis: physiologic tests, quantitative CT indexes, and CT visual scores as predictors of mortality. *Radiology* 2008; **246**: 935–40. doi: https://doi.org/10.1148/radiol.2463062200
162. Jacob J, Bartholmai BJ, Rajagopalan S, Brun AL, Egashira R, Karwoski R, et al. Evaluation of computer-based computer tomography stratification against outcome models in connective tissue disease-related interstitial lung disease: a patient outcome study. *BMC Med* 2016; **14**: 190. doi: https://doi.org/10.1186/s12916-016-0739-7